BRAIN RESEARCH 1621 (2015) 121–132

Available online at www.sciencedirect.com

ScienceDirect

www.elsevier.com/locate/brainres

Brain Research

Research Report

Rapid increase of spines by dihydrotestosterone and testosterone in hippocampal neurons: Dependence on synaptic androgen receptor and kinase networks

Yusuke Hatanaka[a,1], Yasushi Hojo[a,b,1], Hideo Mukai[a,b], Gen Murakami[a,b], Yoshimasa Komatsuzaki[a], Jonghyuk Kim[a], Muneki Ikeda[a], Ayako Hiragushi[a], Tetsuya Kimoto[a], Suguru Kawato[a,b,*]

[a]Department of Biophysics and Life Sciences, Graduate School of Arts and Sciences, The University of Tokyo, 3-8-1 Komaba, Meguro, Tokyo 153-8902, Japan

[b]Bioinformatics Project of Japan Science and Technology Agency, The University of Tokyo, Tokyo, Japan

ARTICLE INFO

Article history:
Accepted 3 December 2014
Available online 13 December 2014

Keywords:
Androgen
Androgen receptor
Dihydrotestosterone
Hippocampus
Spine
Synapse
Testosterone

ABSTRACT

Rapid modulation of hippocampal synaptic plasticity by locally synthesized androgen is important in addition to circulating androgen. Here, we investigated the rapid changes of dendritic spines in response to the elevation of dihydrotestosterone (DHT) and testosterone (T), by using hippocampal slices from adult male rats, in order to clarify whether these signaling processes include synaptic/extranuclear androgen receptor (AR) and activation of kinases. We found that the application of 10 nM DHT and 10 nM T increased the total density of spines by approximately 1.3-fold within 2 h, by imaging Lucifer Yellow-injected CA1 pyramidal neurons. Interestingly, DHT and T increased different head-sized spines. While DHT increased middle- and large-head spines, T increased small-head spines. Androgen-induced spinogenesis was suppressed by individually blocking Erk MAPK, PKA, PKC, p38 MAPK, LIMK or calcineurin. On the other hand, blocking CaMKII did not inhibit spinogenesis. Blocking PI3K altered the spine head diameter distribution, but did not change the total spine density. Blocking mRNA and protein synthesis did not suppress the enhancing effects induced by DHT or T. The enhanced spinogenesis by androgens was blocked by AR antagonist, which AR was localized postsynaptically. Taken together, these results imply that enhanced spinogenesis by DHT and T is mediated by synaptic/extranuclear AR which rapidly drives the kinase networks.

This article is part of a Special Issue entitled SI: Brain and Memory.

*Corresponding author at: Department of Biophysics and Life Sciences, Graduate School of Arts and Sciences, The University of Tokyo, 3-8-1 Komaba, Meguro, Tokyo 153-8902, Japan. Fax: +81 3 5454 6517.
E-mail address: kawato@bio.c.u-tokyo.ac.jp (S. Kawato).

[1]Contributed equally to the present work.

http://dx.doi.org/10.1016/j.brainres.2014.12.011
0006-8993/

1. Introduction

Endogenous synthesis of dihydrotestosterone (DHT) and testosterone (T) has been demonstrated in male rat hippocampal neurons (Hojo et al., 2004). Mass-spectrometric analysis has revealed that the level of adult male hippocampal androgen is higher than that of plasma androgen (Hojo et al., 2009). These results suggest that hippocampal T (~17 nM) may be the sum of hippocampus-synthesized T (~3 nM) and circulating T (~14 nM), which penetrates into the hippocampus. The level of hippocampal DHT is approximately 7 nM which is much higher than that of circulating DHT (~0.6 nM). Therefore, it is important to investigate the modulating effects on synaptic plasticity by hippocampal androgen.

For over a decade, slow modulating effects on synaptic plasticity by circulating androgen have been investigated. Gonadectomy decreases spine–synapses in male rat hippocampus, and the replacement of DHT or T through subcutaneous injection rescues the level of spine–synapse density of CA1 neurons in gonadectomized rats, after three days (Leranth et al., 2003). Electrophysiological investigations in rat hippocampal slices have shown that T application rescues excitatory postsynaptic potentiation (EPSP), which is decreased by castration (Smith et al., 2002). For rats castrated during puberty, T decreases hippocampal long-term potentiation (LTP) in vivo (Harley et al., 2000), and an antagonist of androgen receptor (AR), flutamide, suppresses this reduction (Hebbard et al., 2003). Gonadectomized male rats show impaired cognitive performance, and androgen replacement rescues this impairment (Edinger and Frye, 2004; Frye and Seliga, 2001). A direct application of androgen to the rat hippocampus in vivo has anti-anxiety effects mediated via AR (Edinger and Frye, 2005, 2006).

Candidates of receptors for androgen action have been investigated in the hippocampus. The expression of AR in the hippocampal neurons (Brown et al., 1995; Simerly et al., 1990) implies that the hippocampal neurons are the target of DHT and T. In the CA1 area of the hippocampus, AR appears to be primarily located in the pyramidal neurons (Clancy et al., 1992; Kerr et al., 1995). AR is located not only in the cytoplasm and in the nuclei but also within dendritic spines and axon terminals (Tabori et al., 2005). These results suggest that androgen may have rapid effects on synaptic function via synaptic/extranuclear AR, in addition to slow genomic effect.

Molecular mechanisms of rapid effects of androgen in the hippocampus are, however, still largely unknown (Foradori et al., 2008; Hajszan et al., 2008), in contrast to deep understandings of estrogen-induced rapid synaptic effects. Leranth, MacLusky and their coworkers conclude that remodeling of spine–synapses by androgen is not driven via AR (Hajszan et al., 2008). Our earlier study has shown androgen-induced rapid increase of dendritic thorns in CA3 stratum lucidum via MAPK and PKC, but not via PKA (Hatanaka et al., 2009). The rapid effect of androgen on the spinogenesis may play an important role in memory processes via producing new spines for creating new neuronal contacts. Here, we performed experiments to test the hypothesis that androgen rapidly modulates dendritic spines via nongenomic signaling, including activation of synaptic/extranulear AR and several kinases (including MAPK, PKA, PKC, LIMK). We also investigated different effects of DHT and T on spine head diameter distribution.

2. Results

2.1. *Rapid effect of androgen on CA1 spinogenesis*

We investigated the effect of DHT and T on the modulation of the dendritic spine density and morphology in the hippocampal CA1 stratum radiatum. In addition to T, DHT (non-aromatizable androgen) was also used, because T may be partially converted into estrogen, estradiol (E2), by hippocampal endogenous aromatase (Hojo et al., 2004, 2008). Spine analysis was performed for secondary branches of the apical dendrites located 100–200 μm away from the pyramidal cell body, in the middle of the stratum radiatum of CA1 region.

2.2. *Time-dependence and dose dependence*

Following a 0.5–2 h treatment with DHT or T, treated dendrites significantly have more spines than control dendrites (i.e. with no DHT or T) (Fig. 1A). Time dependency of androgen treatment was demonstrated by treating slices for 0.5, 1 and 2 h with 10 nM DHT or 10 nM T (Fig. S1). The increasing effect on the total spine density was approximately proportional to the incubation time, showing 1.06 (0.5 h), 1.14 (1 h) and 1.28 spines/μm (2 h) in DHT-treatments, and 1.05 (0.5 h), 1.10 (1 h) and 1.32 spines/μm (2 h) in T-treatments. Dose dependency was also observed after 2 h incubation (Fig. S1). In DHT-treatment, the increasing effect on the total spine density was strongest at 10 nM DHT (1.28 spines/μm) as compared with 1 nM (1.17 spines/μm) and 100 nM (1.10 spines/μm) DHT. In T-treatments, the increasing effect was strongest at 10 nM T (1.32 spines/μm) compared with 1 nM T (1.28 spines/μm) and 100 nM T (1.29 spines/μm). Since 2 h treatments with 10 nM DHT and 10 nM T were most effective for spinogenesis, these incubation time and concentration were used in the following investigations unless specified (Fig. S1). Applied concentrations of DHT and T are similar to the concentrations of endogenous hippocampal DHT (~7 nM) and T (~17 nM) (Hojo et al., 2009).

Two hours treatments with 10 nM DHT and 10 nM T increased spines from 0.97 (control, i.e. with no DHT or T) to 1.28 (10 nM DHT) and 1.32 spines/μm (10 nM T). These results indicate that the enhancing effect of spinogenesis by DHT and T is nearly identical for affecting the spine density. Blocking androgen receptor (AR) by 1 μM hydroxyflutamide (HF), a specific inhibitor of AR, completely blocked the increasing effect by DHT and T on the spine density (Fig. 1B).

2.2.1. *Spine head diameter analysis*

The morphological changes in spine head diameter, induced by 2 h treatments, were assessed. We classified the spines into three categories depending on their head diameter: 0.2–0.4 μm as small-head spines, 0.4–0.5 μm as middle-head spines, and 0.5–1.0 μm as large-head spines (Fig. 1C). Small-, middle-, and large-head spines may be different in the number of AMPA receptors, and therefore these three types of spines may have different efficiency in signal transduction. The number of

AMPA receptors (including GluR1 subunit) in the spine increases as the size of postsynapse increases, whereas the number of NMDA receptors (including NR2B subunit) may be relatively constant (Shinohara et al., 2008).

We performed a statistical analysis based on classification of the spines into three categories. In control slices (with no DHT or T), the spine density was 0.41 spines/μm for small-head spines, 0.33 spines/μm for middle-head spines, and 0.25 spines/μm for large-head spines. Upon treatment with DHT, the densities of middle- and large-head spines significantly increased, while the density of small-head spines was not significantly altered (Fig. 1C and D). Upon treatment with T, the density of small-head spines significantly increased, while the density of middle- and large-head spines was not significantly changed (Fig. 1C and D). When compared with only DHT application, co-application of HF with DHT significantly decreased the density of middle- and large-head spines, while the density of small-head spines was not significantly changed (Fig. 1D). When compared with only T

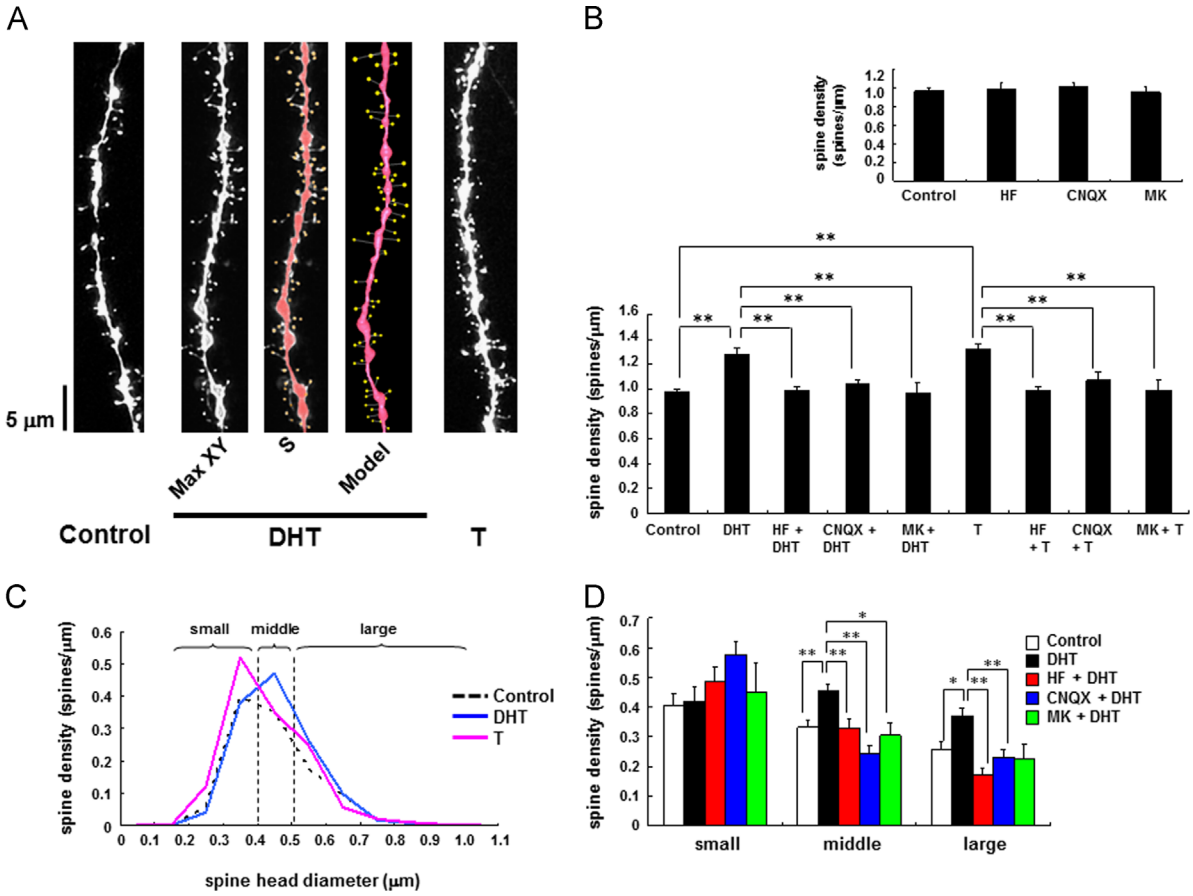

Fig. 1 – Changes in the density and morphology of spines by androgen and blockers in hippocampal slices. (A) Spines were analyzed along the secondary dendrites of pyramidal neurons in the stratum radiatum of CA1 neurons. Maximal intensity projections onto XY plane from z-series confocal micrographs, showing spines along the dendrites of hippocampal CA1 pyramidal neurons. Dendrite without drug-treatment (Control), dendrite after DHT-treatment for 2 h (DHT), and dendrite after T-treatment for 2 h (T). For DHT, image analyzed by Spiso-3D (S) and 3 dimensional model illustration (Model) are also shown. Bar, 5 μm. (B) (Lower) Effect of treatments by DHT, T or receptor blockers on the total spine density in CA1 neurons. (Upper) No effects by blockers alone. Vertical axis is the average number of spines per 1 μm. A 2 h treatment in ACSF without drugs (Control), with 10 nM DHT (DHT), with 10 nM DHT and 1 μM hydroxyflutamide (AR antagonist) (HF+DHT), with 10 nM DHT and 20 μM CNQX (AMPA receptor blocker) (CNQX+DHT), with 10 nM DHT and 50 μ M MK-801 (NMDA receptor blocker) (MK+DHT), with 10 nM T (T), with 10 nM T and 1 μM hydroxyflutamide (HF+T), with 10 nM DHT and 20 μM CNQX (CNQX+T), with 10 nM T and 50 μM MK-801 (MK+T). (C) Histogram of spine head diameters after a 2 h treatment in ACSF without drugs (Control, black dashed line), with 10 nM DHT (blue line), and with 10 nM T (red line). Spines were classified into three categories depending on their head diameter, e.g. smaller than 0.4 μm as small-head spines, 0.4–0.5 μm as middle-head spines, and larger than 0.5 μm as large-head spines. (D) Density of three subtypes of spines. Abbreviations are same as in (B). Vertical axis is the number of spines per 1 μm of dendrite. From left to right, small-head spines (small), middle-head spines (middle), and large-head spines (large). ACSF without drugs (Control, open column), DHT (black column), HF+DHT (red column), CNQX+DHT (blue column), MK+DHT (green column). Results are represented as mean+SEM. Statistical significance yielded $^{*}P<0.05$, $^{**}P<0.01$ vs DHT or T sample. For each drug treatment, we investigated, 3 rats, 8 slices, 16 neurons, 32 dendrites and 1700–2000 spines, except for control, DHT or T which consists of 5 rats, 15 slices, 30 neurons, 60 dendrites and approximately 3000 spines.

application, co-application of HF with T significantly decreased the density of small-head spines, while the densities of middle- and large-head spines were not significantly changed.

2.3. *Effects of glutamate receptor antagonists on androgen-induced spinogenesis*

We investigated the importance of Ca^{2+} concentration for androgen-induced spinogenesis. Since the Ca^{2+} level was maintained by ionotropic glutamate receptors in spines, we examined the spinogenesis in the presence of the following receptor inhibitors. Twenty μM CNQX, an inhibitor of AMPA receptor, and 50 μM MK-801, an NMDA receptor inhibitor, induced a significant decrease in the total spine density (Fig. 1B). These results indicate that the basal spine Ca^{2+} level, maintained by spontaneous opening/closing of AMPA and NMDA receptors, may be necessary for androgen-induced spinogenesis.

The morphological changes in spine head size in the presence of ionotropic glutamate receptor inhibitors were analyzed. In DHT-induced spinogenesis, application of CNQX and MK-801 significantly decreased middle-head spines and large-head spines, but did not decrease the density of small-head spines (Figs. 1D and S3A). On the other hand, in T-induced spinogenesis, application of CNQX and MK-801 abolished the effect of T by decreasing all the three sub-populations of spines (Figs. 1B and S3B).

2.4. *Signaling pathways in androgen-induced spinogenesis depending on protein kinases*

2.4.1. *Total density analysis*

We investigated the intracellular signaling pathways of several kinases involved in the androgen-induced spinogenesis, by using selective inhibitors of kinases (Figs. 2A, E and 3A). Blocking Erk MAPK by application of 25 μM U0126, abolished

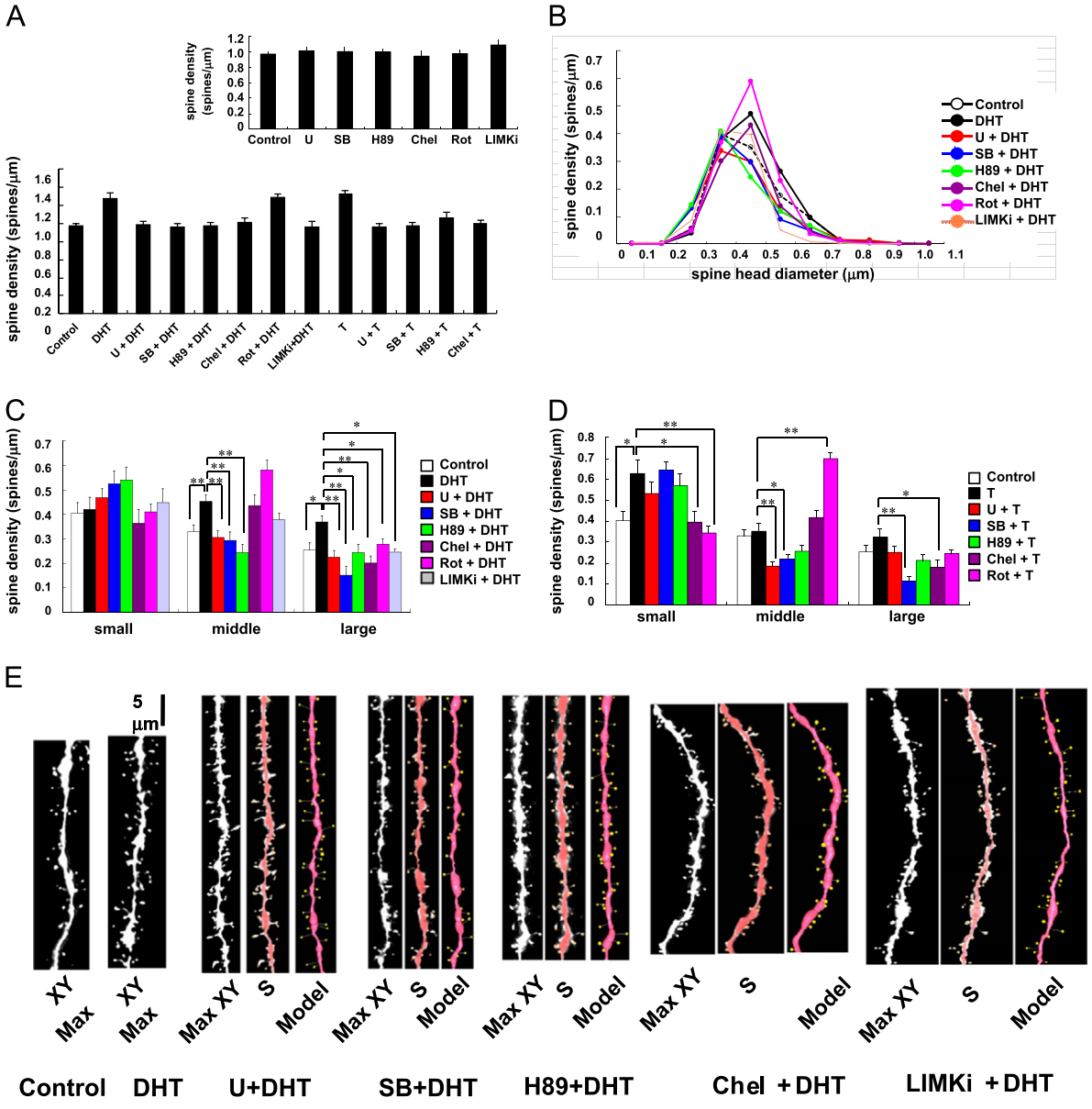

the DHT- and T-effect that increased the total spine density. Application of 10 μM SB203580, a p38 MAPK inhibitor, also prevented the effect by DHT and T. Application of 10 μM H89, an inhibitor of protein kinase A (PKA), blocked the increasing effect by DHT and T. Application of 10 μM LIMKi (Ross-Macdonald et al., 2008), a LIM kinase inhibitor, also prevented the effect by DHT and T. When all subfamilies of protein kinase C (PKC) were blocked by using 10 μM chelerythrine, a non-selective PKC subfamily inhibitor, the increasing effect by DHT and T was blocked. On the other hand, selective inhibition of PKCδ (by 5 μM rottlerin) did not suppress the effect by DHT and T. One μM cyclosporin A (Wiederrecht et al., 1993), an inhibitor of calcineurin (protein phosphatase 2B), abolished the increasing effect by DHT and T. A PI3K inhibitor, 10 μM LY294002 (Vlahos et al., 1994), did not affect the increase of total spine density, which was induced by DHT and T. One μM KN-93, an inhibitor of CaMKII, did not block the effect by DHT and T.

Since the concentrations of inhibitors are added to their recommended concentrations, the inhibitory effects cannot be non-specific due to the excess amount of inhibitors. It should be noted that these kinase inhibitors alone did not significantly affect the total spine density within experimental error, indicating that the observed inhibitory effects are not due to simple blockers' effects (Figs. 2A Upper and S2B).

2.4.2. *Spine head diameter analysis*

Since observing the total spine density dose not tell us enough for understanding the complex kinase effects, the changes in spine head diameter distribution were analyzed. For example, in DHT-treated spines, although the total spine density was not altered by rottlerin, rottlerin decreased the density of large-head spines, but increased middle-head spines (Fig. 2A–C). For DHT-treated spines, LY also decreased the density of middle- and large-head spines without a significant change in the total spine density, because LY increased the density of small-head spines (Fig. 3B and D).

2.4.2.1. DHT and kinase blocking. Inhibitors were co-incubated with 10 nM DHT. Blocking Erk MAPK, p38 MAPK, PKA, LIMK and calcineurin abolished the effect by DHT on the dendritic spine densities, decreasing the density of the middle-head spines and large-head spines, while there were not significant changes in the small-head spines (Figs. 2B, C, 3B and S3C). Inhibiting all the PKC subfamilies and LIM kinase (LIMK) significantly decreased the density of large-head spines, with no changes in the density of small-head spines and middle-head spines (Fig. 2B and C). On the other hand, selective inhibition of PKCδ decreased the density of large-head spines, however, it increased the density of middle-head spines, and did not change small-head spines (Fig. 2B, C). Blocking PI3K decreased the density of middle-head spines and large-head spines, however, it increased small-head spines (Figs. 3B and S3C). It should be noted that although PKCδ and PI3K inhibition did not significantly change the total spine density, these inhibitions altered the subpopulations of spines. Blocking CaMKII, which did not change the total spine density, also showed no effect on the subpopulations of spines (Figs. 3B and S3C).

2.4.2.2. T and kinase blocking. Inhibiting Erk MAPK abolished the effect of T on the dendritic spine density, decreasing the density of middle-head spines (from 0.35 to 0.19 spines/μm), while there were not significant changes in small-head spines and large-head spines (Fig. 2D). Individually blocking p38 MAPK and calcineurin significantly decreased the density of middle-head spines and large-head spines, while

Fig. 2 – Effects of inhibition by kinase inhibitors on changes in the density and morphology of spines by DHT and T. Spines were analyzed along the secondary dendrites of CA1 pyramidal neurons as in Fig. 1. (A) (Lower) Effect of kinase inhibitors in the presence of DHT or T on the total spine density in CA1 neurons. (Upper) No effects by kinase inhibitors alone. Vertical axis is the average number of spines per 1 μm. A 2 h treatment in ACSF without drugs (Control), with 10 nM DHT (DHT), with 10 nM DHT and 25 μM U0126 (Erk MAPK inhibitor) (U+DHT), with 10 nM DHT and 10 μM SB203580 (p38 MAPK inhibitor) (SB+DHT), with 10 nM DHT and 10 μM H-89 (PKA inhibitor) (H89+DHT), with 10 nM DHT and 10 μM chelerythrine (PKC inhibitor) (Chel+DHT), with 10 nM DHT and 5 μM rottlerin (PKCδ inhibitor) (Rot+DHT), and with 10 nM DHT and 10 μM LIMKi (LIMK inhibitor) (LIMKi+DHT), with 10 nM T (T), with 10 nM T and 25 μM U0126 (U+T), with 10 nM T and 10 μM SB203580 (SB+T), with 10 nM T and 10 μM H-89 (H89+T), with 10 nM T and 10 μM chelerythrine (Chel+T). (B) Histogram of spine head diameters. Abbreviations are same as in (A). Vertical axis is the number of spines per 1 μm of dendrite. A 2 h treatment in ACSF without drugs (Control, dashed line), with DHT (black line), with U+DHT (red line), with SB+DHT (blue line), with H89+DHT (green line), with Chel+DHT (purple line), with Rot+DHT (pink line), and with LIMKi+DHT (orange line). (C) Density of three subtypes of spines. Abbreviations are same as in (A). Vertical axis is the average number of spines per 1 μm of dendrite. From left to right, small-head spines (small), middle-head spines (middle), and large-head spines (large). In each group, control (open column), DHT (black column), U+DHT (red column), SB+DHT (blue column), H89+DHT (green column), Chel+DHT (purple column), Rot+DHT (pink column), and LIMKi+DHT (gray column). (D) Density of three subtypes of spines. Abbreviations are same as in (A). Vertical axis is the average number of spines per 1 μm of dendrite. From left to right, small-head spines (small), middle-head spines (middle), and large-head spines (large). In each group, control (open column), T (black column), U+T (red column), SB+T (blue column), H89+T (green column), Chel+T (purple column), and Rot+T (pink column). (E) Representative spine images of confocal micrographs used for (A)–(C): DHT plus U treatment (U+DHT); DHT plus SB treatment (SB+DHT); DHT plus H89 treatment (H89+DHT); DHT plus chelerythrine treatment (Chel+DHT); DHT and LIMKi (LIMK inhibitor) (LIMKi+DHT). Maximal intensity projection onto XY plane from z-series (Max-XY), image analyzed by Spiso-3D (S) and 3 dimensional model (Model) are shown together. Bar, 5 μm. In (A), (C), and (D) results are represented as mean ± SEM. Statistical significance yielded $^{*}P<0.05$, $^{**}P<0.01$ vs DHT or T sample. For each drug treatment, we investigated 3 rats, 8 slices, 16 neurons, 32 dendrites and 1700–2000 spines.

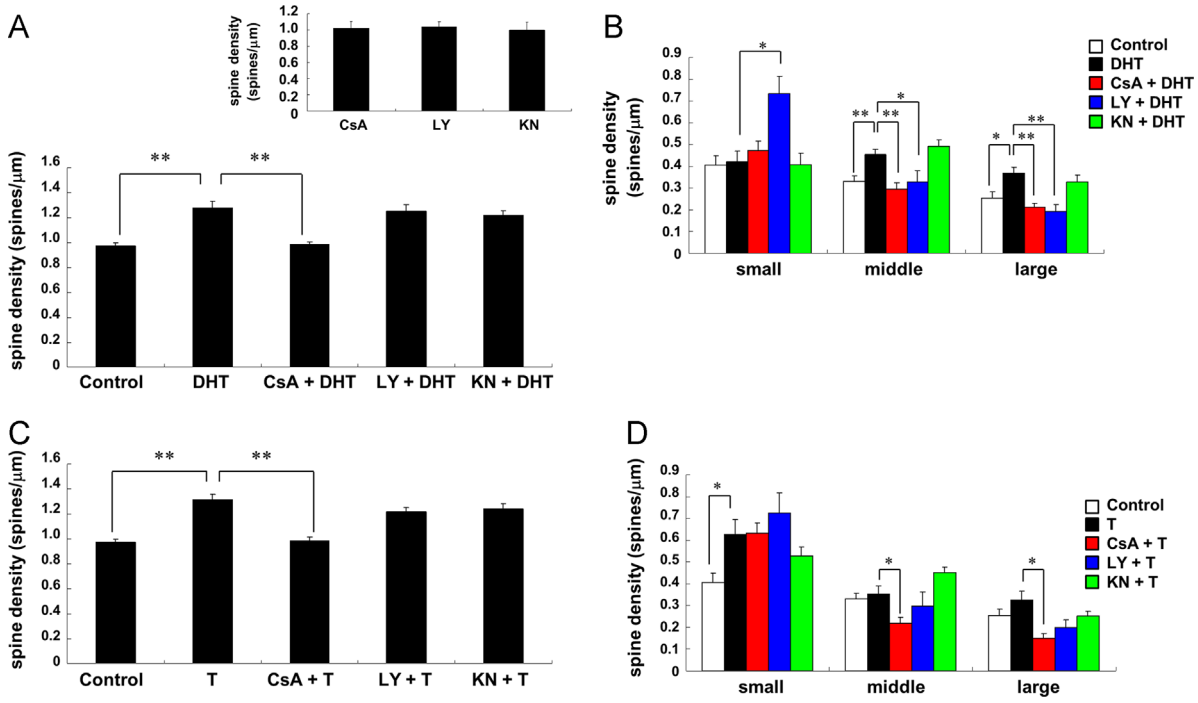

Fig. 3 – Effects of inhibition by phosphatase and kinases on changes in the density and morphology of spines by DHT and T. Spines were analyzed along the secondary dendrites of CA1 pyramidal neurons as in Fig. 1. (A) (Lower) Effect of inhibitors in the presence of DHT on the total spine density in CA1 neurons. (Upper) No effects by kinase inhibitors alone. Vertical axis is the average number of spines per 1 μm. A 2 h treatment in ACSF without drugs (Control), with 10 nM DHT (DHT), with 10 nM DHT and 1 μM cyclosporin A (calcineurin inhibitor) (CsA+DHT), with 10 nM DHT and 10 μM LY294002 (PI3K inhibitor) (LY+DHT), and with 10 nM DHT and 1 μM KN-93 (CaMKII inhibitor) (KN+DHT). (B) Density of three subtypes of spines. Abbreviations are same as in (A). Vertical axis is the average number of spines per 1 μm of dendrite. From left to right, small-head spines (small), middle-head spines (middle), and large-head spines (large). In each group, control (open column), DHT (black column), CsA+DHT (red column), LY+DHT (blue column), and KN+DHT (green column). (C) Effect of kinase inhibitors in the presence of T on the total spine density in CA1 neurons. Vertical axis is the average number of spines per 1 μm. A 2 h treatment in ACSF without drugs (Control), with 10 nM T (T), with 10 nM T and 1 μM cyclosporin A (CsA+T), with 10 nM T and 10 μM LY294002 (LY+T), and with 10 nM T and 1 μM KN-93 (KN+T). (D) Density of three subtypes of spines. Abbreviations are same as in (A). Vertical axis is the average number of spines per 1 μm of dendrite. From left to right, small-head spines (small), middle-head spines (middle), and large-head spines (large). ACSF without drugs (Control, open column), T (black column), CsA+T (red column), LY+T (blue column), and KN+T (green column). Results are reported as mean ± SEM. Statistical significance yielded $^{*}P<0.05$, $^{**}P<0.01$ vs DHT or T sample. For each drug treatment, we investigated 3 rats, 7 slices, 14 neurons, 28 dendrites and 1400–1700 spines.

small-head spines showed no changes in its density (Fig. 2D). Blocking PKA moderately decreased the density of middle-head spines and large-head spines (Fig. 2D). Inhibition of all the PKC subfamilies significantly decreased the density of small-head spines and large-head spines, with few changes in middle-head spines (Fig. 2D). On the other hands, selectively blocking PKCδ decreased the density of small-head spines, while it increased middle-head spines with few changes in large-head spines (Fig. 2D). It should be noted that although PKCδ inhibition did not significantly change the total spine density, PKCδ inhibition altered the distribution of spine head diameter. Blocking PI3K, which also did not change the total spine density, showed no effect on all the three subpopulations of spines (Fig. 3C and D). Inhibiting CaMKII, which did not change the total spine density, also showed no effect on all the three subpopulations of spines (Fig. 3C and D).

2.5. *Blocking mRNA and protein synthesis in androgen-induced spinogenesis*

The total density of spines (in the presence of DHT or T) was not altered by the presence of 4 μM actinomycin D (ActD), a mRNA synthesis inhibitor, or by the presence of 20 μM cycloheximide (CHX), a protein synthesis inhibitor (Fig. 4). These results suggest that DHT- and T-induced spinogenesis is non-genomic process.

2.6. *No contribution of T-metabolites (E2 and DHT) to T-induced spinogenesis*

In order to exclude the possibility that the effect of T may be a mixed effect of T with its metabolites, which are E2 (converted by cytochrome P450arom) and DHT (converted by 5α-reductase), we co-applied letrozole (P450arom inhibitor) with

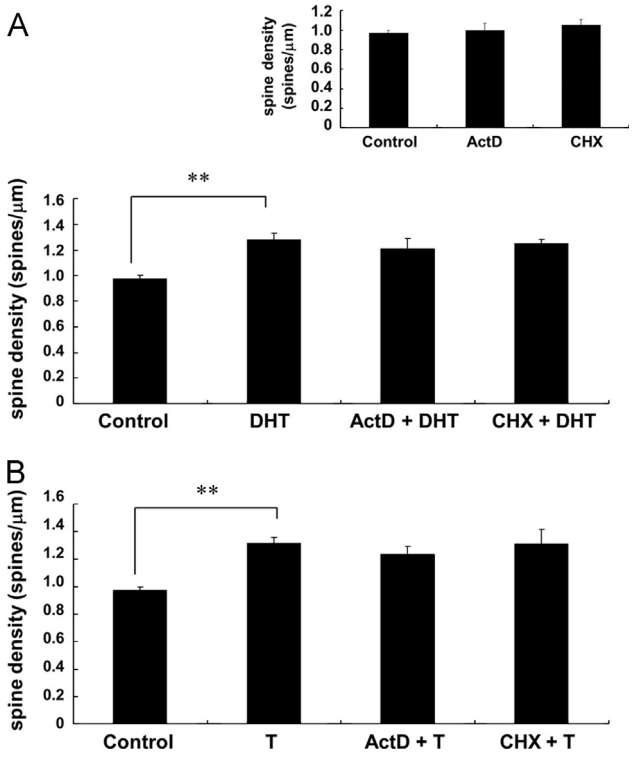

Fig. 4 – No effects by inhibition of mRNA and protein synthesis on changes in the total density of spines by DHT and T. Spines were analyzed along the secondary dendrites of CA1 pyramidal neurons as in Fig. 1. (A) (Lower) No effects by mRNA and protein synthesis inhibitors in the presence of DHT on the total spine density in CA1 neurons. (Upper) No effects of inhibitors alone. Vertical axis is the average number of spines per 1 μm. A 2 h treatment in ACSF without drugs (Control), with 10 nM DHT (DHT), with 10 nM DHT and 4 μM actinomycin D (transcription inhibitor) (ActD+DHT), and with 10 nM DHT and 20 μM cycloheximide (translation inhibitor) (CHX+DHT) are shown. (B) No effects by mRNA and protein synthesis inhibitors in the presence of T on the total spine density. Vertical axis is the average number of spines per 1 μm. A 2 h treatment in ACSF without drugs (Control), with 10 nM T (T), with 10 nM T and 4 μM actinomycin D (ActD+T), and with 10 nM T and 20 μM cycloheximide (CHX+T). Results are reported as mean ± SEM. Statistical significance yielded $^{*}P<0.05$, $^{**}P<0.01$ vs DHT or T sample. For each drug treatment, we investigated 3 rats, 6 slices, 12 neurons, 24 dendrites and 1300–1500 spines.

T, and finasteride (5α-reductase inhibitor) with T. Both 100 nM letrozole and 1 μM finasteride did not suppress the increasing effect by T on the total spine density, implying that the conversion from T to E2 or from T to DHT did not occur within 2 h (Fig. S4).

2.7. *Localization of AR in spines*

Since androgen-induced rapid spinogenesis suggests the involvement of AR (which localizes at spines) during the rapid spinogenesis, we used Western immunoblot analysis in order to elucidate the subcellular distribution of AR. Using anti-AR antibody, PG-21 (1/1000 dilution), a protein band was observed, with a molecular mass of approximately 110 kDa, in PSD fraction as well as in cytoplasmic and nuclear fractions (Fig. S5).

3. Discussion

3.1. *Rapid effect of androgen on spine density and morphology*

3.1.1. *Difference between DHT and T*

We observed different rapid effects by DHT and T treatments, modulating the spine density and morphology of the hippocampal CA1 neurons. DHT treatments dramatically increased the density of middle-head spines and large-head spines. In contrast, small-head spines were increased by T treatments (Figs. 1C, D and 2D). Large-head spines have significantly more AMPA receptors than small-head spines (Shinohara et al., 2008). These results suggest that DHT may increase more memory-related synaptic activities than T. This T-effect, or increase of small-head spines is not due to the conversion from T to E2, and neither from T to DHT. This is because T-effect was not inhibited by blockade of P450arom (E2 synthetase) and 5α-reductase (DHT synthetase). Furthermore, the effect of T was blocked by AR antagonist. Therefore, we conclude that T-effect is directly mediated by AR, and not mediated by E2 (T-metabolite). It should be noted that DHT and T differently affect spine head diameters, although they both increased the total spine density to almost the same extent. DHT possess the stronger effects than T on spine head diameter, which might be caused by their difference in triggering different kinases. For example, T may drive PKC for increase of small-head spines, and DHT may drive PKA and MAPK for increase of middle-head spines, as suggested in inhibitor experiments (Fig. 2C and D). In earlier study, DHT has been shown to have more potent androgenic effects than T, and DHT has approximately three fold higher affinity than T for AR (Breiner et al., 1986).

3.1.2. *Kinase-mediated signaling in spinogenesis (Fig. 5)*

The current results from kinase inhibitions imply that the rapid effects by both DHT and T were mediated by serine/threonine kinases, including MAPK, PKA, and PKC (Fig. 2). Since both AR and these kinases/phosphatase are present in spines, an efficient coupling between these proteins could occur at postsynapses (Mukai et al., 2007; Tabori et al., 2005).

In CA1 region, MAPK cascade is known for associating with PKA and PKC via PKC→Raf1→Erk MAPK, PKA→B-Raf→Erk MAPK in synaptic modulation including LTP (Roberson et al., 1999). Therefore, MAPK may be the main kinase that is responsible for the modulation of spines. Androgens rapidly phosphorylate Erk MAPK (Fix et al., 2004; Gatson et al., 2006) and PKC (Sato et al., 2008) via AR in a variety of tissues. PKA activation, via androgen-AR pathway, has not been reported previously. PKA is activated by androgens; however, its action is mediated by flutamide-independent androgen receptor in prostate cells (Bagchi et al., 2008).

In spine reorganization, the target of Erk MAPK may be cortactin. Erk MAPK is known for phosphorylating cortactin,

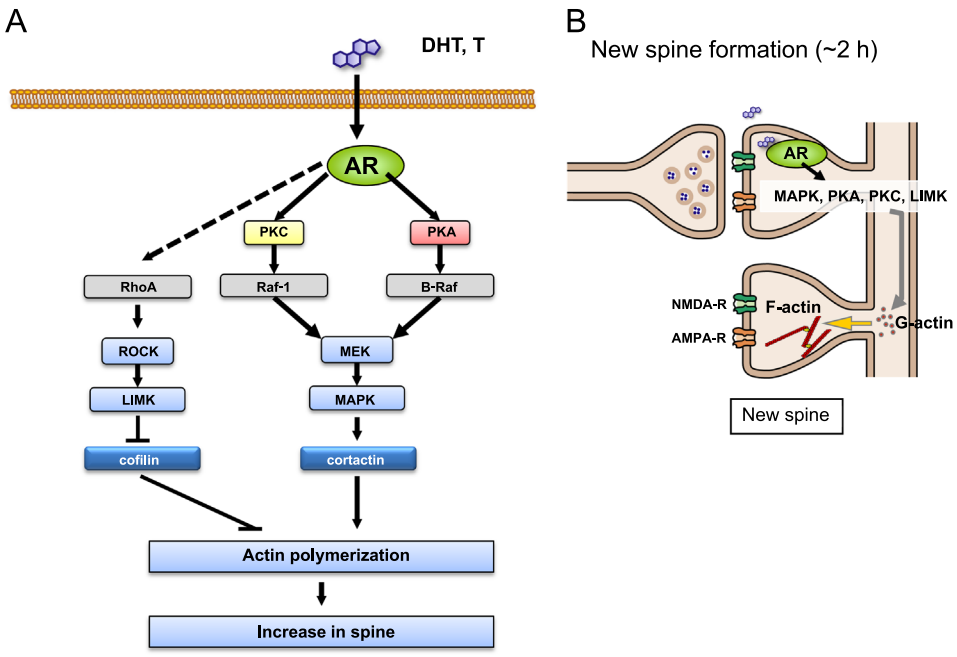

Fig. 5 – Schematic illustration for androgen-induced spine formation mediated by AR and its downstream kinase networks.

a structural protein associated with actin (MacQueen et al., 2003). Cortactin interacts with F-actin, actin-related protein (Arp) 2/3 complex, and Shank, the scaffold protein, in the PSD at the SH3 domain (Campbell et al., 1999; Weed et al., 1998). The combination of these proteins results in promotion of actin fiber remodeling within spines. For example, upon BDNF stimulation, MAPK phosphorylates cortactin by interacting C-terminal of SH3 domain, reorganizing the spine morphology (Iki et al., 2005). It is thus possible that DHT and T may exert their effects on spines via cortactin-actin pathway. Cortactin has multiple phosphorylation sites, including Ser^{405} and Ser^{418}, which are activated by MAPK (Campbell et al., 1999). Phosphorylation of cortactin may promote grouping actin cytoskeletal matrices, which can either lead to forming spines or modulating the spine morphology (Hering and Sheng, 2003). These sites and also Ser^{113} are putative phosphorylation sites for other serine/threonine kinase (PKA or PKC) that are either activated by DHT or T. The involvement of cortactin in androgen-induced modulation of spines can be suggested from the fact that flutamide induces actin depolymerization via tyrosine phosphorylation of cortactin (Anahara et al., 2006). Interestingly, the effect from the administration of DHT and T was completely blocked by excluding only one member of kinases, although many kinases participate in androgen-induced spinogenesis (Fig. 2). These results suggest that completing androgen-induced spinogenesis may need multiple phosphorylation of cortactin. In this case, whenever a single phosphorylation is blocked, spinogenesis may not be accomplished (Fig. 2).

LIMK and cofilin are also good candidates for androgen-induced actin reassembly, leading to spinogenesis (see Fig. 2) (Clancy et al., 1992; Liston et al., 2013; Sato et al., 2008). It is known that corticosterone induces the phosphorylation of both LIMK and cofilin, leading to spinogenesis (Liston et al., 2013). Cofilin polymerizes actin filaments upon phosphorylation by LIMK (Clancy et al., 1992). PKC or RhoA may phosphorylate LIMK (Pilpel and Segal, 2004; Shi et al., 2009).

In a previous study, we demonstrated that androgen (DHT or T) induces rapid increase of CA3 thorns. These events mediated via Erk MAPK, p38 MAPK, PKCs, calcineurin, and CaMKII (Hatanaka et al., 2009). The thorns are postsynaptic sites of mossy fiber terminals in CA3. Interestingly, although PKA is involved in androgen-induced spinogenesis in CA1 (Fig. 2), PKA does not cause androgen-induced thorn-genesis in CA3. CaMKII is not involved in androgen-induced spinogenesis in CA1 (Fig. 3), however, CaMKII contributes androgen-induced thorn-genesis in CA3. These results imply the differences in involvement of kinases in CA1 and CA3. PI3K was not involved in androgen-induced spinogenesis in both CA1 and CA3.

3.2. *Action of AR in spinogenesis*

We observed that AR was localized at PSD of neurons in addition to cytoplasm and nuclei (Fig. S5). Immunoelectron microscopic analysis have demonstrated that AR is localized not only in cytoplasm and nuclei but also inside of spines (Tabori et al., 2005). AR protein and AR mRNA are expressed significantly in CA1 hippocampal neurons (Kerr et al., 1995; Xiao and Jordan, 2002). These results support the idea that AR localized within spines may mediate androgen-induced rapid spinogenesis by activating several kinases.

3.3. *Earlier studies of rapid AR action*

So far, two types of different mechanisms of rapid androgen actions have been considered (Foradori et al., 2008): (Type 1) nuclear AR mediated signaling in hipocampal neurons, and (Type 2) non-AR type androgen receptor (non-AR) mediated signaling that is not blocked by AR antagonist. For type 1

mechanism, 10 nM DHT and T individually phosphorylates Erk MAPK followed by phosphorylations of Rsk1 and Bad within 1 h, creating neuroprotection against amyloid β in primary cultured hippocampal neurons (Nguyen et al., 2005). As for type 2 mechanism, T-BSA (non-membrane permeable testosterone) activates non-AR in LNCaP cells, and then triggers Rho small GTPases, LIMK2, and destrin, which leads to actin polymerization (Papadopoulou et al., 2008). Destrin belongs to a family of cofilin, which is known as an important factor for spine formation. For peripheral cells, there are several other studies, reporting the rapid action of androgen through non-AR (Estrada et al., 2003; Papakonstanti et al., 2003). In this study, rapid spinogenesis enhancement by androgen was blocked by hydroxyflutamide, an AR-specific antagonist, therefore the rapid androgen-induced spinogenesis is type 1.

3.4. *In vivo effects of androgen*

A number of in vivo studies have been concerned about the effect of gonadal androgen supplement (DHT or T: 500 μg/d, s.c.), mostly for observing on the recovery of spine–synapse density of the hippocampal pyramidal cells for gonadectomized male rats (Kovacs et al., 2003; Leranth et al., 2003; MacLusky et al., 2006). In gonadectomized male rats, circulating androgen is undetectable, and the spine–synapse density decreases significantly. Spine–synapses are spines which form synpases with presynapses observed by electron micrograph (Leranth et al., 2003). Leranth, MacLusky and colleagues have demonstrated that the rescue effects of androgens on CA1 spine–synapse formation are not blocked by flutamide, an AR antagonist, in gonadectomized rats (Leranth et al., 2004). Surprisingly, flutamide supplementation increased the spine–synapse density. The rescue effects of the spine–synapse density by DHT and flutamide were also observed in gonadectomized Tfm (testicular feminization mutant) male rats that are deficient in AR (MacLusky et al., 2006). These results suggest that the effects of androgens on spine–synapses may be mediated through non-AR type receptor (Hajszan et al., 2008; MacLusky et al., 2006). In our research, the effects of androgen on CA1 spines, in hippocampal slices, were clearly blocked by hydroxyflutamide. This difference of AR involvement might be due to the difference in mechanisms between chronic in vivo action (spine–synapse) and rapid action in isolated hippocampal slices, or between spine–synapse formation and dendritic spine formation.

Androgen also affects anxiety and fear. Androgen application on the hippocampus, injected 48 h prior to the tasks, inhibits increased anxiety behaviors of gonadectomized rats (Edinger and Frye, 2004, 2005). These androgen-induced anxiolytic actions are mediated through AR (Edinger and Frye, 2006).

It should be noted that the mechanisms of androgen action may be different between in vivo and in vitro experiments, because indirect effects of androgen may also occur in vivo via cholinergic or serotonergic neurons, projecting to the hippocampus, in addition to direct influence of androgen on glutamatergic neurons (Kovacs et al., 2003). Moreover, gonadectomy, which is necessary to avoid contribution of plasma androgen, may change the condition of the cholinergic, serotonergic or glutamatergic neurons to be of shortage of androgen, and therefore, the supplement of T propionate had such a significant impact.

3.5. *Differences between androgen and estrogen in rapid synaptic effects*

E2 is known for inducing rapid CA1 spinogenesis via Erk MAPK (Luine and Frankfurt, 2012; Mukai et al., 2007; Phan et al., 2011). There are differences between androgen and estrogen actions. Although DHT-induced spinogenesis did not include PI3K pathway (Figs. 3 and S3C), E2 induces spinogenesis via PI3K pathway (Hasegawa et al., 2015). PI3K has some specific interactions with E2 signaling. For example, PI3K directly binds to estrogen receptor (Simoncini et al., 2000), and PI3K mediates E2-induced acute neuroprotection from apoptotic cell death, caused by ischemia in the hippocampal CA1 region (Jover-Mengual et al., 2010). Protein synthesis was not involved in androgen-induced spinogenesis (Fig. 4), but it is required for E2-induced spinogenesis (Mukai et al., 2007).

In CA3 region, clear differences between DHT and E2 were observed during spinogenesis. DHT increased the density of thorns (spine-like postsynaptic structure in CA3) (Hatanaka et al., 2009); however, E2 decreased the thorn density (Tsurugizawa et al., 2005).

3.6. *Androgen levels in the hippocampus*

In the hippocampus, DHT and T should play a major role as a rapid modulator of synaptic plasticity via synaptic AR. The concentration of endogenous DHT and T is determined to be approx. 7 nM and 17 nM, respectively, in a freshly isolated hippocampus by mass-spectrometric analysis (Hojo et al., 2008, 2009). However, it should be noted that in order to obtain 'acute' slices (normally used for analysis of synaptic plasticity) by recovery-incubation of hippocampal slices with ACSF, the levels of DHT and T decreased to below 0.5 nM (Fig. S6) (Hojo et al., 2011). In this study, the exogenous application of 10 nM DHT and 10 nM T was individually used to elevate the hippocampal androgen level from the steroid-depleted level in 'acute' slice (<0.5 nM), rapidly back to the endogenous level. Exogenous application of DHT and T was employed to modulate hippocampal androgen levels, because until now the method of rapid elevation of endogenous androgen concentration via activation of its synthesis enzymes is not yet established. The effect of kinase inhibitors alone was not seen, because androgens (<0.5 nM) were depleted in acute slices by incubation in ACSF (Fig. 2). In such acute slices without androgens, AR and kinases are probably not endogenously activated. In physiological conditions in vivo, hippocampal DHT and T (7 nM and 17 nM) may significantly regulate AR, several kinases and spines.

To investigate in a more intrinsic condition, the methods of rapid activation of endogenous synthesis of androgen should be developed, referring from the NMDA-induced synthesis (Hojo et al., 2004; Kawato et al., 2002), or possibly synthesis by using 1–10 Hz low frequency electric stimulation.

4. Experimental procedures

4.1. *Animals*

Twelve-week-old adult male Wistar rats were purchased from Saitama Experimental Animal Supply. All experimental

procedures of this research were approved by the Committee for Animal Research of Univ of Tokyo.

4.2. Chemicals

Cyano-nitroquinoxaline-dione (CNQX), Cyclosporin A, dihydrotestosterone, Lucifer Yellow CH, LY-294,002, SB-203580, SP600125, testosterone, U0126, MK-801, actinomycin D, and cycloheximide, were purchased from Sigma (USA). Chelerythrine, KN-93, rottlerin, LIMKi were purchased from Calbiochem (USA). H-89 was purchased from Biomol (USA). Hydroxyflutamide was purchased from Wako Pure Chamicals (Japan).

4.3. Imaging and analysis of dendritic spine density and morphology

4.3.1. Hipocampal slice preparation and current injection of Lucifer Yellow

Male rats aged 12 weeks were deeply anesthetized and decapitated. The brains were removed and placed in artificial cerebrospinal fluid (ACSF) at 4 °C. ACSF consisted of (mM): 124 NaCl, 5.0 KCl, 1.25 NaH_2PO_4, 2.0 $MgSO_4$, 2.0 $CaCl_2$, 22 $NaHCO_3$, and 10 glucose, and was equilibrated with 95% O_2/5% CO_2. The hippocampus was dissected and 300 μm transverse slices to the long axis from the middle third of the hippocampus were cut with a vibratome (Dosaka, Japan). These 'fresh' hippocampal slices were transferred into an incubating chamber containing ACSF held at 25 °C for 2 h for slice recovery. Resultant 'acute' slices (used worldwide) were then incubated with 0.1–10 nM DHT or T together with inhibitors of protein kinases, ion channels, or protein synthesis (Fig. S6). Slices were then fixed with 4% paraformaldehyde in PBS at 4 °C overnight. Neurons within slices were visualized by an injection of Lucifer Yellow (Molecular Probes, USA) under Nikon E600FN microscope (Japan) equipped with a C2400-79H infrared camera (Hamamatsu Photonics, Japan) and with a 40× water immersion lens (Nikon, Japan). Current injection was performed with glass electrode filled with 5% Lucifer Yellow for 15 min, using Axopatch 200B (Axon Instruments, USA). Approximately five neurons within a depth of 100–200 μm from the surface of a slice were injected with Lucifer Yellow (Duan et al., 2002).

4.3.2. Confocal laser microscopy and morphological analysis

The imaging was performed from sequential z-series scans with confocal laser scan microscope (LSM5; Carl Zeiss, Germany) at high zoom (×3.0) with a 63× water immersion lens, NA 1.2. For Lucifer Yellow, the excitation and emission wavelengths were 488 nm and 515 nm, respectively. For analysis of spines, three-dimensional image was reconstructed from approximately 40 sequential z-series sections of every 0.45 μm with a 63× water immersion lens, NA 1.2. The applied zoom factor (×3.0) yielded 23 pixel per 1 μm. The z-axis resolution was approximately 0.71 μm. The confocal lateral resolution was approximately 0.26 μm. Our resolution limits were regarded to be sufficient to allow the determination of the density of spines. Confocal images were then deconvoluted using AutoDeblur software (AutoQuant, USA).

The density of spines as well as the head diameter was analyzed with Spiso-3D (automated software mathematically calculating geometrical parameters of spines) developed by Bioinformatics Project of Kawato's group (Mukai et al., 2011). Spiso-3D has an equivalent capacity with Neurolucida (MicroBrightField, USA), furthermore, Spiso-3D considerably reduces human errors and experimenter labor. The single apical dendrite was analyzed separately. The spine density was calculated from the number of spines along secondary dendrites having a total length of 40–70 μm. These dendrites were present within the stratum radiatum, between 100 and 200 μm from the soma. Spine shapes were classified into three categories as follows. (1) A small-head spine, whose head diameter is smaller than 0.4 μm. (2) A middle-head spine, which has 0.4–0.5 μm spine head. (3) A large-head spine, whose head diameter is larger than 0.5 μm. These three categories were useful to distinguish different responses upon kinase inhibitor application. Since the majority of spines (>95%) had a distinct head and neck, and stubby spines and filopodia did not contribute much to overall changes, we analyzed spines, having a distinct head.

4.4. Preparation of synaptic, cytoplasmic and nuclear fractions

Adult male rats were deeply anesthetized and decapitated. The brains were removed and placed in ACSF. Slices were homogenized in 0.32 M sucrose in 1 mM $NaHCO_3$, 1 mM $MgCl_2$, 0.5 mM $CaCl_2$ with protease inhibitors 0.5 mM PMSF and 0.1 mM leupeptin, and centrifuged at 1400*g* for 10 min. The pellet was centrifuged again in the same solution. The pellet was used as the nuclear fraction (P1 fraction). Supernatant from the first centrifugation was subjected to centrifugation at 10,000*g* for 20 min. The retrieved pellet (P2 fraction) was further purified with sucrose density gradient centrifugation. The pellet was suspended in 0.32 M sucrose in 1 mM $NaHCO_3$ and overlaid on 0.85/1.0/1.2 M sucrose step gradient. The sample was ultracentrifuged at 82,500*g* for 120 min. The synaptosomal fraction was collected from the interface between 1.0 M and 1.2 M sucrose. Purification of the 'PSD fraction' was performed as follows. Synaptosomal fraction was treated with 1% Triton X-100 in 12 mM Tris–HCl (pH 8.1), and Triton-insoluble pellet fraction was collected by centrifugation at 32,800*g* for 20 min. The pellet was suspended in 0.32 M sucrose in 1 mM $NaHCO_3$ and overlaid on 1.0/1.5/2.1 M sucrose step gradient. The sample was ultracentrifuged at 201,800*g* for 120 min. Crude PSD fraction was collected from the interface between 1.5 M and 2.1 M sucrose, and then suspended in 150 mM KCl with 1% TritonX-100. The suspension was centrifuged for 20 min at 201,800*g*, and the pellet was collected as purified PSD fraction. To obtain the 'presynaptic membrane-enriched fraction' (low density synaptic membrane fraction), the supernatant obtained from fractionation of P2 was centrifuged at 25,000*g* for 60 min. Resultant supernatant was centrifuged again at 100,000*g* for 60 min, and the pellet and the supernatant were collected separately as the presynaptic membrane-enriched fraction and the cytoplasmic fraction, respectively.

4.5. Western immunoblot analysis

Purified fractions, prepared by centrifugation, were suspended in 125 mM Tris–HCl buffer (pH 6.8), containing 5 mM 2-mercaptoethanol, 10% sucrose, 6% sodium dodecylsulfate

and 0.002% bromophenol blue. The fractions were subjected to electrophoresis using a 10% polyacrylamide gel. After transfer to polyvinylidene fluoride membranes (Immobilon-P; Millipore Co., USA), the blots were probed with anti-androgen receptor, PG-21 (Upstate) (diluted to 1/1000) for 12–18 h at 4 °C, and incubated with horseradish peroxidase (HRP) conjugated goat anti-rabbit IgG (Cell Signaling). The protein bands were detected with ECL plus Western blotting detection reagents (Amersham, USA). To obtain high quality images of chemiluminescence from protein bands using ECL plus, we used LAS3000 Image Analyzer (Fuji Film, Japan) with a 16-bit wide dynamic range.

4.6. *Statistical analysis*

The significance of DHT, T, or drug effect was examined via statistical analysis using Tukey-Kramer post-hoc multiple comparisons test when one-way ANOVA tests yielded $P<0.05$.

Acknowledgements

We thank Mr. Taishi Takeda (Rutgers Univ.) for his critical reading the manuscript.

Appendix A. Supporting information

Supplementary data associated with this article can be found in the online version at http://dx.doi.org/10.1016/j.brainres.2014.12.011.

REFERENCES

Anahara, R., Toyama, Y., Maekawa, M., Yoshida, M., Kai, M., Ishino, F., Toshimori, K., Mori, C., 2006. Anti-estrogen ICI 182.780 and anti-androgen flutamide induce tyrosine phosphorylation of cortactin in the ectoplasmic specialization between the Sertoli cell and spermatids in the mouse testis. Biochem. Biophys. Res. Commun. 346, 276–280.

Bagchi, G., Wu, J., French, J., Kim, J., Moniri, N.H., Daaka, Y., 2008. Androgens transduce the G alphas-mediated activation of protein kinase A in prostate cells. Cancer Res. 68, 3225–3231.

Breiner, M., Romalo, G., Schweikert, H.U., 1986. Inhibition of androgen receptor binding by natural and synthetic steroids in cultured human genital skin fibroblasts. Klin. Wochenschr. 64, 732–737.

Brown, T.J., Sharma, M., Heisler, L.E., Karsan, N., Walters, M.J., MacLusky, N.J., 1995. In vitro labeling of gonadal steroid hormone receptors in brain tissue sections. Steroids 60, 726–737.

Campbell, D.H., Sutherland, R.L., Daly, R.J., 1999. Signaling pathways and structural domains required for phosphorylation of EMS1/cortactin. Cancer Res. 59, 5376–5385.

Clancy, A.N., Bonsall, R.W., Michael, R.P., 1992. Immunohistochemical labeling of androgen receptors in the brain of rat and monkey. Life Sci. 50, 409–417.

Duan, H., Wearne, S.L., Morrison, J.H., Hof, P.R., 2002. Quantitative analysis of the dendritic morphology of corticocortical projection neurons in the macaque monkey association cortex. Neuroscience 114, 349–359.

Edinger, K.L., Frye, C.A., 2004. Testosterone's analgesic, anxiolytic, and cognitive-enhancing effects may be due in part to actions of its 5alpha-reduced metabolites in the hippocampus. Behav. Neurosci. 118, 1352–1364.

Edinger, K.L., Frye, C.A., 2005. Testosterone's anti-anxiety and analgesic effects may be due in part to actions of its 5alpha-reduced metabolites in the hippocampus. Psychoneuroendocrinology 30, 418–430.

Edinger, K.L., Frye, C.A., 2006. Intrahippocampal administration of an androgen receptor antagonist, flutamide, can increase anxiety-like behavior in intact and DHT-replaced male rats. Horm. Behav. 50, 216–222.

Estrada, M., Espinosa, A., Muller, M., Jaimovich, E., 2003. Testosterone stimulates intracellular calcium release and mitogen-activated protein kinases via a G protein-coupled receptor in skeletal muscle cells. Endocrinology 144, 3586–3597.

Fix, C., Jordan, C., Cano, P., Walker, W.H., 2004. Testosterone activates mitogen-activated protein kinase and the cAMP response element binding protein transcription factor in Sertoli cells. Proc. Natl. Acad. Sci. U.S.A 101, 10919–10924.

Foradori, C.D., Weiser, M.J., Handa, R.J., 2008. Non-genomic actions of androgens. Front. Neuroendocrinol. 29, 169–181.

Frye, C.A., Seliga, A.M., 2001. Testosterone increases analgesia, anxiolysis, and cognitive performance of male rats. Cogn. Affect. Behav. Neurosci. 1, 371–381.

Gatson, J.W., Kaur, P., Singh, M., 2006. Dihydrotestosterone differentially modulates the mitogen-activated protein kinase and the phosphoinositide 3-kinase/Akt pathways through the nuclear and novel membrane androgen receptor in C6 cells. Endocrinology 147, 2028–2034.

Hajszan, T., MacLusky, N.J., Leranth, C., 2008. Role of androgens and the androgen receptor in remodeling of spine synapses in limbic brain areas. Horm. Behav. 53, 638–646.

Harley, C.W., Malsbury, C.W., Squires, A., Brown, R.A., 2000. Testosterone decreases CA1 plasticity in vivo in gonadectomized male rats. Hippocampus 10, 693–697.

Hasegawa, Y., Hojo, Y., Kojima, Y., Ikeda, Y., Hotta, K., Sato, R., Ooishi, Y., Yoshiya, M., Chung, B.C., Yamazaki, T., Kawato, S., 2015. Estradiol Rapidly Modulates Synaptic Plasticity of Hippocampal Neurons: Involvement of Kinase Networks. Brain Res. 1621, 147–161, http://dx.doi.org/10.1016/j.brainres.2014.12.056.

Hatanaka, Y., Mukai, H., Mitsuhashi, K., Hojo, Y., Murakami, G., Komatsuzaki, Y., Sato, R., Kawato, S., 2009. Androgen rapidly increases dendritic thorns of CA3 neurons in male rat hippocampus. Biochem. Biophys. Res. Commun. 381, 728–732.

Hebbard, P.C., King, R.R., Malsbury, C.W., Harley, C.W., 2003. Two organizational effects of pubertal testosterone in male rats: transient social memory and a shift away from long-term potentiation following a tetanus in hippocampal CA1. Exp. Neurol. 182, 470–475.

Hering, H., Sheng, M., 2003. Activity-dependent redistribution and essential role of cortactin in dendritic spine morphogenesis. J. Neurosci. 23, 11759–11769.

Hojo, Y., Hattori, T.A., Enami, T., Furukawa, A., Suzuki, K., Ishii, H.T., Mukai, H., Morrison, J.H., Janssen, W.G., Kominami, S., Harada, N., Kimoto, T., Kawato, S., 2004. Adult male rat hippocampus synthesizes estradiol from pregnenolone by cytochromes P45017alpha and P450 aromatase localized in neurons. Proc. Natl. Acad. Sci. U.S.A 101, 865–870.

Hojo, Y., Murakami, G., Mukai, H., Higo, S., Hatanaka, Y., Ogiue-Ikeda, M., Ishii, H., Kimoto, T., Kawato, S., 2008. Estrogen synthesis in the brain–role in synaptic plasticity and memory. Mol. Cell. Endocrinol. 290, 31–43.

Hojo, Y., Higo, S., Ishii, H., Ooishi, Y., Mukai, H., Murakami, G., Kominami, T., Kimoto, T., Honma, S., Poirier, D., Kawato, S., 2009. Comparison between hippocampus-synthesized and

circulation-derived sex steroids in the hippocampus. Endocrinology 150, 5106–5112.
Hojo, Y., Higo, S., Kawato, S., Hatanaka, Y., Ooishi, Y., Murakami, G., Ishii, H., Komatsuzaki, Y., Ogiue-Ikeda, M., Mukai, H., Kimoto, T., 2011. Hippocampal synthesis of sex steroids and corticosteroids: essential for modulation of synaptic plasticity. Front. Endocrinol. (Lausanne) 2, 43.
Iki, J., Inoue, A., Bito, H., Okabe, S., 2005. Bi-directional regulation of postsynaptic cortactin distribution by BDNF and NMDA receptor activity. Eur. J. Neurosci. 22, 2985–2994.
Jover-Mengual, T., Miyawaki, T., Latuszek, A., Alborch, E., Zukin, R.S., Etgen, A.M., 2010. Acute estradiol protects CA1 neurons from ischemia-induced apoptotic cell death via the PI3K/Akt pathway. Brain Res. 1321, 1–12.
Kawato, S., Hojo, Y., Kimoto, T., 2002. Histological and metabolism analysis of P450 expression in the brain. Methods Enzymol. 357, 241–249.
Kerr, J.E., Allore, R.J., Beck, S.G., Handa, R.J., 1995. Distribution and hormonal regulation of androgen receptor (AR) and AR messenger ribonucleic acid in the rat hippocampus. Endocrinology 136, 3213–3221.
Kovacs, E.G., MacLusky, N.J., Leranth, C., 2003. Effects of testosterone on hippocampal CA1 spine synaptic density in the male rat are inhibited by fimbria/fornix transection. Neuroscience 122, 807–810.
Leranth, C., Petnehazy, O., MacLusky, N.J., 2003. Gonadal hormones affect spine synaptic density in the CA1 hippocampal subfield of male rats. J. Neurosci. 23, 1588–1592.
Leranth, C., Hajszan, T., MacLusky, N.J., 2004. Androgens increase spine synapse density in the CA1 hippocampal subfield of ovariectomized female rats. J. Neurosci. 24, 495–499.
Liston, C., Cichon, J.M., Jeanneteau, F., Jia, Z., Chao, M.V., Gan, W.B., 2013. Circadian glucocorticoid oscillations promote learning-dependent synapse formation and maintenance. Nat. Neurosci. 16, 698–705.
Luine, V.N., Frankfurt, M., 2012. Estrogens facilitate memory processing through membrane mediated mechanisms and alterations in spine density. Front. Neuroendocrinol. 33, 388–402.
MacLusky, N.J., Hajszan, T., Johansen, J.A., Jordan, C.L., Leranth, C., 2006. Androgen effects on hippocampal CA1 spine synapse numbers are retained in Tfm male rats with defective androgen receptors. Endocrinology 147, 2392–2398.
MacQueen, G.M., Campbell, S., McEwen, B.S., Macdonald, K., Amano, S., Joffe, R.T., Nahmias, C., Young, L.T., 2003. Course of illness, hippocampal function, and hippocampal volume in major depression. Proc. Natl. Acad. Sci. U.S.A 100, 1387–1392.
Mukai, H., Tsurugizawa, T., Murakami, G., Kominami, S., Ishii, H., Ogiue-Ikeda, M., Takata, N., Tanabe, N., Furukawa, A., Hojo, Y., Ooishi, Y., Morrison, J.H., Janssen, W.G., Rose, J.A., Chambon, P., Kato, S., Izumi, S., Yamazaki, T., Kimoto, T., Kawato, S., 2007. Rapid modulation of long-term depression and spinogenesis via synaptic estrogen receptors in hippocampal principal neurons. J. Neurochem. 100, 950–967.
Mukai, H., Hatanaka, Y., Mitsuhashi, K., Hojo, Y., Komatsuzaki, Y., Sato, R., Murakami, G., Kimoto, T., Kawato, S., 2011. Automated analysis of spines from confocal laser microscopy images: application to the discrimination of androgen and estrogen effects on spinogenesis. Cerebral Cortex 21, 2704–2711.
Nguyen, T.V., Yao, M., Pike, C.J., 2005. Androgens activate mitogen-activated protein kinase signaling: role in neuroprotection. J. Neurochem. 94, 1639–1651.
Papadopoulou, N., Charalampopoulos, I., Alevizopoulos, K., Gravanis, A., Stournaras, C., 2008. Rho/ROCK/actin signaling regulates membrane androgen receptor induced apoptosis in prostate cancer cells. Exp. Cell Res. 314, 3162–3174.
Papakonstanti, E.A., Kampa, M., Castanas, E., Stournaras, C., 2003. A rapid, nongenomic, signaling pathway regulates the actin reorganization induced by activation of membrane testosterone receptors. Mol. Endocrinol. 17, 870–881.
Phan, A., Lancaster, K.E., Armstrong, J.N., MacLusky, N.J., Choleris, E., 2011. Rapid effects of estrogen receptor alpha and beta selective agonists on learning and dendritic spines in female mice. Endocrinology 152, 1492–1502.
Pilpel, Y., Segal, M., 2004. Activation of PKC induces rapid morphological plasticity in dendrites of hippocampal neurons via Rac and Rho-dependent mechanisms. Eur. J. Neurosci. 19, 3151–3164.
Roberson, E.D., English, J.D., Adams, J.P., Selcher, J.C., Kondratick, C., Sweatt, J.D., 1999. The mitogen-activated protein kinase cascade couples PKA and PKC to cAMP response element binding protein phosphorylation in area CA1 of hippocampus. J. Neurosci. 19, 4337–4348.
Ross-Macdonald, P., de Silva, H., Guo, Q., Xiao, H., Hung, C.Y., Penhallow, B., Markwalder, J., He, L., Attar, R.M., Lin, T.A., Seitz, S., Tilford, C., Wardwell-Swanson, J., Jackson, D., 2008. Identification of a nonkinase target mediating cytotoxicity of novel kinase inhibitors. Mol. Cancer Ther. 7, 3490–3498.
Sato, K., Iemitsu, M., Aizawa, K., Ajisaka, R., 2008. Testosterone and DHEA activate the glucose metabolism-related signaling pathway in skeletal muscle. Am. J. Physiol. Endocrinol. Metab. 294, E961–E968.
Shi, Y., Pontrello, C.G., DeFea, K.A., Reichardt, L.F., Ethell, I.M., 2009. Focal adhesion kinase acts downstream of EphB receptors to maintain mature dendritic spines by regulating cofilin activity. J. Neurosci. 29, 8129–8142.
Shinohara, Y., Hirase, H., Watanabe, M., Itakura, M., Takahashi, M., Shigemoto, R., 2008. Left-right asymmetry of the hippocampal synapses with differential subunit allocation of glutamate receptors. Proc. Natl. Acad. Sci. U.S.A 105, 19498–19503.
Simerly, R.B., Chang, C., Muramatsu, M., Swanson, L.W., 1990. Distribution of androgen and estrogen receptor mRNA-containing cells in the rat brain: an in situ hybridization study. J. Comp. Neurol. 294, 76–95.
Simoncini, T., Hafezi-Moghadam, A., Brazil, D.P., Ley, K., Chin, W.W., Liao, J.K., 2000. Interaction of oestrogen receptor with the regulatory subunit of phosphatidylinositol-3-OH kinase. Nature 407, 538–541.
Smith, M.D., Jones, L.S., Wilson, M.A., 2002. Sex differences in hippocampal slice excitability: role of testosterone. Neuroscience 109, 517–530.
Tabori, N.E., Stewart, L.S., Znamensky, V., Romeo, R.D., Alves, S.E., McEwen, B.S., Milner, T.A., 2005. Ultrastructural evidence that androgen receptors are located at extranuclear sites in the rat hippocampal formation. Neuroscience 130, 151–163.
Tsurugizawa, T., Mukai, H., Tanabe, N., Murakami, G., Hojo, Y., Kominami, S., Mitsuhashi, K., Komatsuzaki, Y., Morrison, J.H., Janssen, W.G., Kimoto, T., Kawato, S., 2005. Estrogen induces rapid decrease in dendritic thorns of CA3 pyramidal neurons in adult male rat hippocampus. Biochem. Biophys. Res. Commun. 337, 1345–1352.
Vlahos, C.J., Matter, W.F., Hui, K.Y., Brown, R.F., 1994. A specific inhibitor of phosphatidylinositol 3-kinase, 2-(4-morpholinyl)-8-phenyl-4H-1-benzopyran-4-one (LY294002). J. Biol. Chem. 269, 5241–5248.
Weed, S.A., Du, Y., Parsons, J.T., 1998. Translocation of cortactin to the cell periphery is mediated by the small GTPase Rac1. J. Cell Sci. 111 (Pt 16), 2433–2443.
Wiederrecht, G., Lam, E., Hung, S., Martin, M., Sigal, N., 1993. The mechanism of action of FK-506 and cyclosporin A. Ann. N.Y. Acad. Sci 696, 9–19.
Xiao, L., Jordan, C.L., 2002. Sex differences, laterality, and hormonal regulation of androgen receptor immunoreactivity in rat hippocampus. Horm. Behav. 42, 327–336.